Mixed convection between two horizontal concentric cylinders when the cooled outer cylinder is rotating

M.A. Teamah, M.M. Sorour and Ramzy A. Saleh
Mechanical Eng. Dept., Faculty of Eng., Alexandria University, Alexandria, Egypt

The objective of the present investigation is to study the laminar combined heat transfer between infinite isothermal horizontal cylinders. The cooled outer cylinder is considered rotating with constant angular speed while the hot inner cylinder is fixed. A mathematical model is constructed and solved numerically. This investigation covers wide ranges of Rayleigh number from 10^3 to 10^6, Reynolds from 0 to 2000, Prantdl from 0.01 to 10, and the ratio of inner diameter to gap width from 0.5 to 5. Three flow patterns were identified according to the number of eddies: two eddies, one eddy, and no eddy. The flow regimes are plotted, and characteristics of flow patterns are elucidated. A comparison is made with the previous investigations. The comparison shows a good agreement with published results.

يحتوى هذا البحث على دراسة عددية لانتقال الحرارة بالحمل الرقائقى المختلط بين اسطوانتين أفقيتين لانهائيتين دائرتى المقطع متحدتى المحور منتظمتى درجة الحرارة بحيث تكون الاسطوانة الخارجية مبردة والاسطوانة الداخلية مسخنة ٠ ويتواجد هذا النظام فى كثير من التطبيقات الصناعية والهندسية ٠ ويتم انتقال الحرارة بالحمل الرقائقى بثلاثة طرق وهى الحمل الطبيعى والحمل الجبرى والحمل المختلط (الطبيعى و الجبرى) وقد تم استعراض ما تم إنجازه فى الأبحاث السابقة والتى تعرضت لكل من انتقال الحرارة بالحمل الطبيعى والحمل المختلط بين اسطوانتين أفقيتين متحدتى المحور وتم عرض القيم الخاصة بكل بحث وعلى ضوء ذلك تم تحديد القيم البحثية التى تم دراستها خلال هذا البحث والتى لم تتعرض لها الأبحاث السابقة وهى ٠ ≥ Re ≥ ٢٠٠٠ و ١٠ ≥ Ra ≥ 10^3 و 10^6 ≥ Pr ≥ ٠,٠١ و ٥ ≥ σ ≥ ٠,٥ هذا وقد تم البدء من المعدلات التفاضلية الرئيسية الخاصة بالسريان و كمية الحركة وانتقال الحرارة فى المحاور الرئيسية الثلاثة: الإتجاه الطولى و الإتجاه القطرى واتجاه الزاوية وقد تم اختصار تلك المعادلات لحلها فى اتجاهين فقط وهما الاتجاه القطرى و اتجاه الزاوية وتم وضعها بعد ذلك فى صورة لا بعدية كى تكون فى صورة عامة وتم حلها بعد ذلك عدديا باستخدام الحاسب الآلى٠ وقد تم استعراض النتائج الخاصة بالبحث والتى تشير إلى وجود ثلاثة مناطق وهى: منطقة الدوامتين و منطقة الدوامة الواحدة و منطقة عدم وجود الدوامات و قد تم عمل مقارنة بين نتائج البحث و النتائج البحثية التى تم الحصول عليها من أبحاث سابقة و وجد أن هناك توافقا كبيرا بينها.

Keywords: Heat transfer, Mixed convection, Horizontal, Rotating annulus

1. Introduction

The laminar convection between two horizontal concentric cylinders is an important problem in heat transfer and fluid flow due to its theoretical interest, and its wide engineering applications such as power transmission cables, sleeves, power chains, journal bearings, and grinding machines.

Comprehensive reviews on the study of natural convection phenomena were presented by Beckmann [1]. Iton et al. [2] correlated the average Nusselt number as a function of the modified Grashof number Gr_m. Kuehn and Goldstein [3] correlated relation for overall Nusselt number for heat transfer by natural convection between an inner and outer cylinder. Singh and Elliott [4] investigated the free convection problem between two concentric horizontal cylinders when the modified Grashof number (Gr_m) is small. Transient natural convection heat transfer problem between two horizontal isothermal cylinders was solved numerically by Tsui, and Tremblay [5]. Rao et al. [6] investigated numerically flow patterns. Prud et al. [7] studied the laminar natural convection in a non-uniformly heated annular fluid layer. Morgan [8] correlated two equations for the Nusselt number in the enclosure between two horizontal cylinders when diameter ratio, R ≥ 10 in the two cases of constant heat flux, and constant temperature on the inner cylinder. Kumar [9] obtained the mean Nusselt number for natural convection in horizontal annuli in a wide range of Ra. Kolesnikov, et al. [10] investigated the problem of non-stationary conjugate free convection heat transfer in horizontal cylindrical coaxial

channels. A computational analysis of steady laminar natural convection of cooled water within a horizontal annulus with constant heat flux on the inner wall and a fixed temperature on the outer surface was presented by Ho et al. [11]. The investigations were made to explore the occurrence of density inversion of water and its effects on the flow and temperature fields. Yoo [12] investigated the transition and multiplicity of flows in natural convection in a narrow horizontal cylindrical annulus. Yoo [13] investigated also the natural convection in a narrow horizontal cylindrical annulus for low Pr. Yoo [14] investigated also the Prandtl number effect on bifurcation and dual solution in natural convection in a horizontal annulus.

Comprehensive review on the study of mixed convection phenomena in horizontal concentric annulus was numerically investigated for air and presented by Yoo[15]. Investigations were made for various combinations of Ra ≤ $5*10^4$, Pr = 0.7, Re ≤ 1500, and σ from 0.5 to 5. The flow patterns can be categorized into three types according to the number of eddies: two-one- and no- eddy flows.

From the previous review, the combined convection heat transfer between two concentric horizontal rotating cylinders was not examined in wide ranges of Reynolds and Rayleigh numbers as well as for few different Prandtl numbers. Therefore, this work investigates the combined heat transfer between two horizontal concentric rotating cylinders numerically. Also this investigation studies wide ranges for Rayleigh number, $0 \le Ra \le 10^6$, Reynolds number, $0 \le Re \le 4000$, inner diameter/ gab width ratio, $0.5 \le \sigma \le 5.0$, and Prantdl number , $0.01 \le Pr \le 10$.

2. Mathematical model

The geometry of the problem is shown in fig. 1. The two cylinders are held at constant different temperatures of T_i and T_o ($T_i > T_o$). The cooled outer cylinder is rotating with constant angular speed in the counter clock-wise direction, and the hot inner cylinder is fixed. Applying the Boussinesq approximation and assuming no slip and isothermal conditions on the cylinders solid surfaces. The equations governing the continuity, momentum and thermal energy in the cylindrical coordinate are formulated into dimensionless form by using the following dimensionless variables:

$$R = \frac{r}{L},\ \theta = \left(\frac{T - T_o}{T_i - T_o}\right),\ P^* = \frac{p}{\rho U^2}\ ,$$

and $\tau = \frac{t}{\rho U^2}$. (1)

The dimensionless governing equations are:

$$\nabla . V = 0\ , \tag{2}$$

$$(V.\nabla)\, V = -\nabla P + \frac{1}{\mathrm{Re}}\nabla^2 V + \frac{Ra}{\mathrm{Pr}\,\mathrm{Re}^2}\theta[\cos(\varphi)e_r - \sin(\varphi)e_\varphi]\ , \tag{3}$$

$$(V.\nabla)\theta = \frac{1}{\mathrm{Pr}\,\mathrm{Re}}\nabla^2\theta\ , \tag{4}$$

the boundary conditions are:

at $R = R_i$ $u = v = 0.0$, $\theta = 1$, (5)

at $R = R_o$ $u = 0.0$, $v = 1$, $\theta = 0.0$. (6)

2.1. Nusselt number calculation

Equating the heat transfer by convection to the heat transfer by conduction gives:

$$h_\varphi \Delta T = -K\frac{\partial T}{\partial r} \qquad \text{when } r=r_i\ . \tag{7}$$

Introducing the dimensionless variables, defined in eq. (1) , into eq. (7), gives:

$$Nu(i) = -\frac{\partial\theta}{\partial R} \qquad \text{when } R=R_i\ . \tag{8}$$

The average Nusselt number around the inner cylinder perimeter is obtained by integrating the above local Nusselt number over the cylinder perimeter:

$$NU_i = \frac{h_i(d_i)}{k} = \frac{1}{2\pi}\sum_0^{2\pi}\left(-\frac{\partial\theta}{\partial R}\right)\Delta\phi \text{ when } R=R_i\ . \tag{9}$$

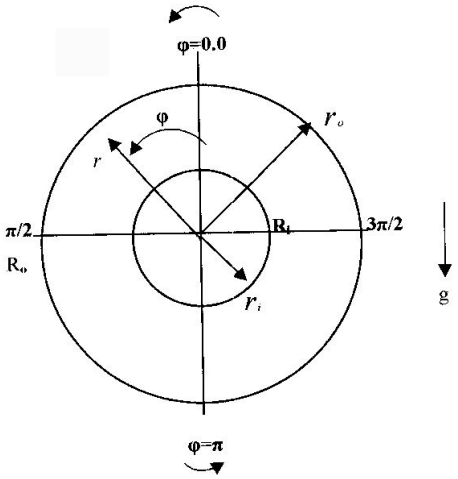

Fig. 1. Problem configuration.

Also the average Nusselt number around the outer cylinder perimeter can be obtained by the same way:

$$NU_o = \frac{h_o(d_o)}{k} = \frac{1}{2\pi}\sum_{0}^{2\pi}\left(-\frac{\partial\theta}{\partial R}\right)\Delta\phi \text{ when } R=R_o. \quad (10)$$

2.2. Shear stress calculation

The sheer stress acting on inner cylinder is given by:

$$t = \mu\frac{\partial_{\upsilon_\varphi}}{\partial r} \text{ when } r=r_i\,. \quad (11)$$

Applying the dimensionless form on the above equation, the dimensionless shear stress is given by:

$$\tau = \frac{t}{\rho U^2} = \frac{1}{\mathrm{Re}}\frac{\partial\upsilon}{\partial R} \text{ when } R=R_o. \quad (12)$$

The number of nodes used was checked. Through-out this study, the number of grids (52 × 47) was used. The 52-grid points in the radial direction are enough to resolve the thin boundary layer near both the two cylinders sufficiently. Finite volume technique developed by Patankar and Spalding [16] was used, which is based on the discretization of the governing equations using the central differencing in space. The discretized equations were solved by the Gauss-seidel method. The iteration method used in this program is a line-by-line procedure, which is a combination of the direct method and the resulting Tri Diagonal Matrix Algorithm (TDMA). The accuracy was defined by the change in the average Nusselt number through one hundred iterations to be less than 0.01 % from its value. The numerical results showed that 2000 iterations were enough for all of the investigated values.

3. Results and discussions

3.1. Hydrodynamic flow results and discussions

Fig. 2 and 3 present samples of the flow patterns at discrete values of Re for different Ra, and Pr. Fig. 2 presents the flow patterns for very small Pr (Pr = 0.01). At Re=0.0(pure natural convection), the flow field is induced by pure buoyancy force, and consists of two kidney- shaped eddies. Both eddies circulate in an opposite direction to each other. When the outer cylinder starts to rotate, the flow pattern looses its symmetry. The variation of flow patterns with respect to Re is shown in fig. 2-a for Ra = 100. For small Re, the two symmetric eddies created by the pure buoyancy force are slightly altered by the forced convection. In the region of $\pi < \varphi < 2\pi$, the forced flow near the outer cylinder opposes the buoyancy induced flow. As Re is increased, the left eddy grows, while the right eddy shrinked, and the flow pattern moves towards one eddy. This pattern persisted with increasing Re within the range of investigation. It is noticed that for condition of pure natural convection, the separation line is located at the vertical axis of annulus. As Re is increased, the separation line at the upper portion moves in the same direction of rotation. As buoyancy forces increase, for Ra= 10^3 to Ra= 10^5, Re has a similar effect on the growth of one eddy and the decay of the other one, but it doesn't disappear within range of investigation. On the other hand, for $0.1 \le Pr \le 10$, and small Ra, with increasing speed of rotation, the flow pattern changes from two eddies to one eddy and ended with no eddy as shown in fig. 3-a. However, as Ra is increased, the circulation of

the fluid between the two cylinders becomes complex. This is caused by the increased drag of buoyancy force.

3.1.1. Effect of gab width on the streamlines

The cases of σ = 0.5 (wide gap) and σ =5 (narrow gap) are presented in fig. 4 for Pr =1.0. In wide gap, the convective fluid flow has more space to move and the fluid motion characteristics tend to be more convective. On the other hand, for narrow gap, the fluid has less space to move and the fluid motion and behavior tend to be more conductive. It is to be noted that the case of wide gap is similar to a single cylinder, and the case of narrow gap is similar to two parallel plates. Also, as shown in fig. 2 to fig. 4, the flows can be categorized into three different patterns according to the number of eddies: i- two eddies, ii- one eddy, and iii- no eddy.

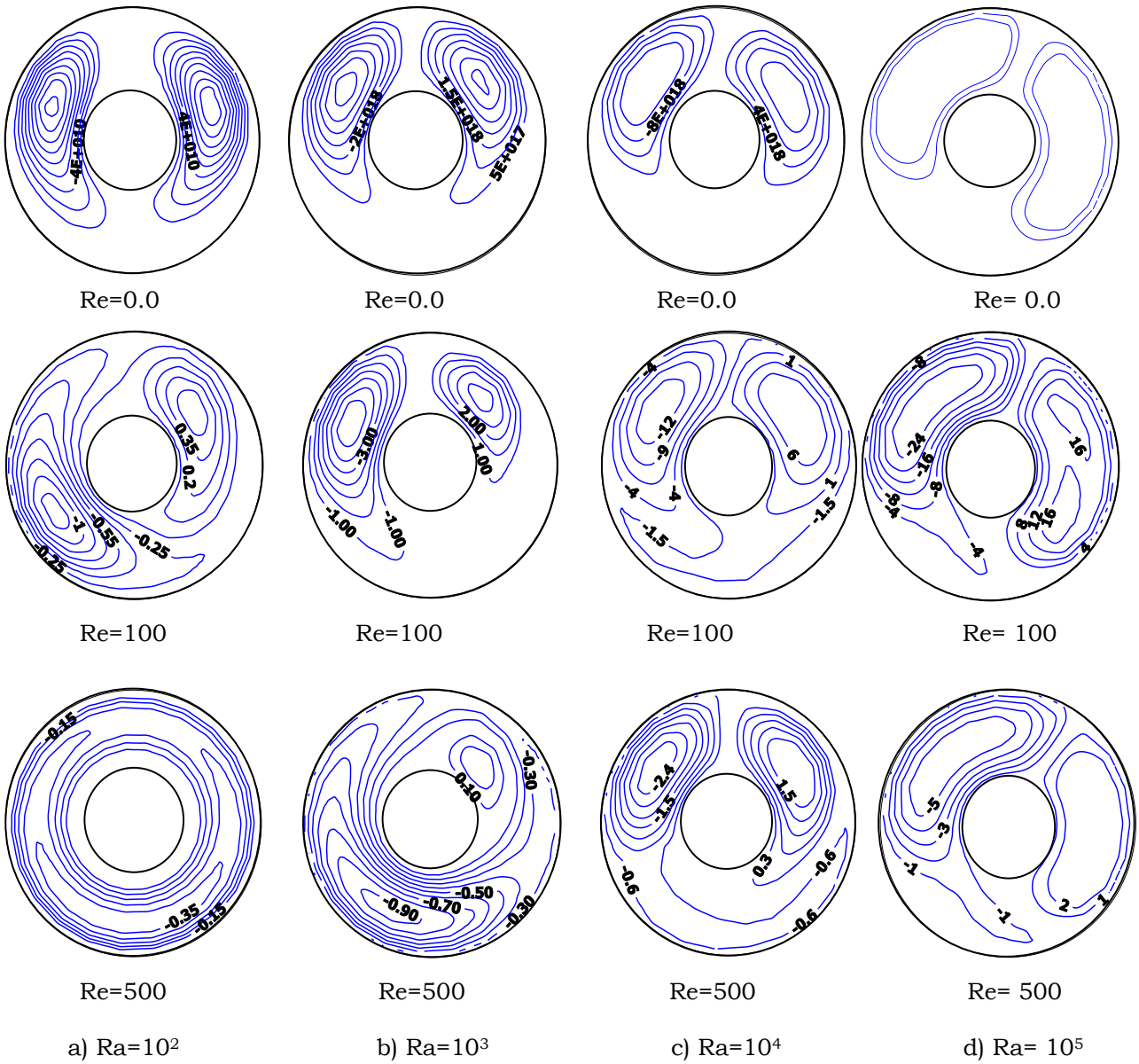

Fig. 2. Flow patterns for different Re, and Ra when σ = 2.0, Pr = 0.01.

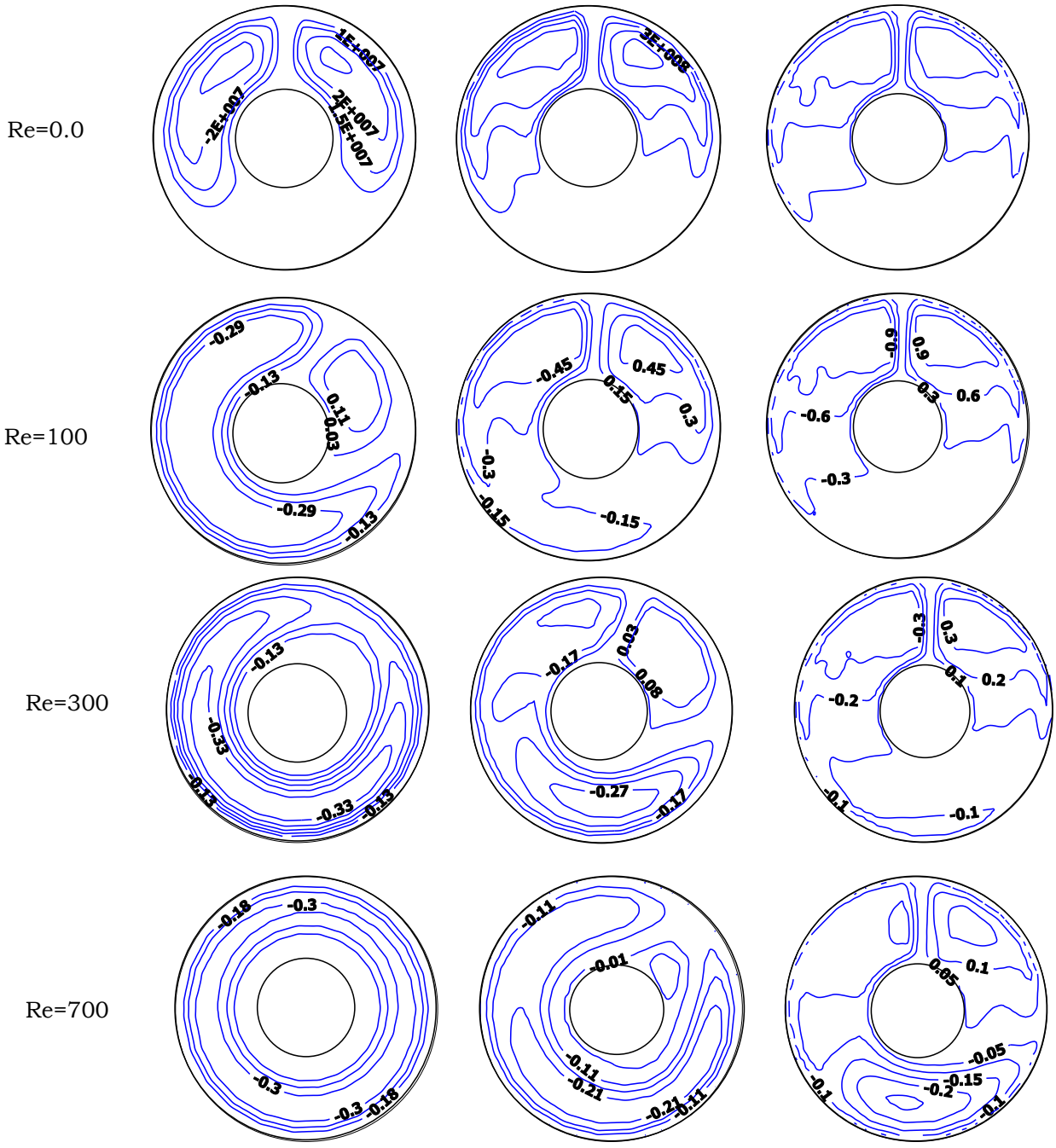

Fig. 3. Flow patterns for several Re, and Ra when σ = 2, Pr =1.0.

3.1.2. Hydrodynamic critical Reynolds number

There are hydrodynamic critical values of Re defining the pattern onset between one eddy and no eddy, and between two eddies and one eddy. Fig. 5 shows the maps of the three flow regimes. From the figure, it can be seen that, the onset is dependent on both Pr, and Ra.

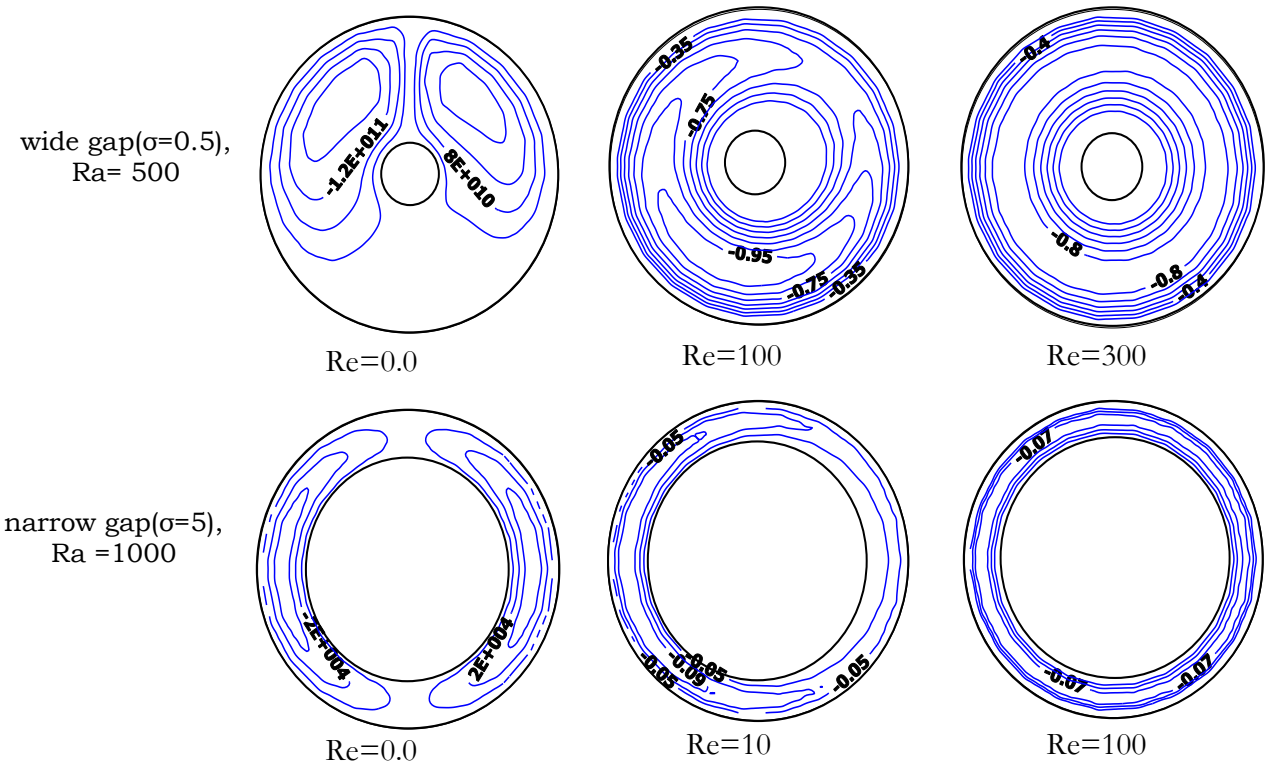

Fig. 4. Flow patterns for several Re, and Ra for wide gap(σ = 0.5), and narrow gap(σ = 5) when Pr =1.0.

3.1.3. The shear stress

The shear stress acting on the inner cylinder is calculated using eq. (12). Fig. 6 shows the shear stress (τ) as a function of Re for different Ra and Pr =1.0 at σ = 2. For all values of Re, as Ra is increased, the shear stress increases due to the strong resisting buoyancy force. It is noticed that, as Re is increased, there is an initial rapid decrease in shear stress followed by a moderate decrease. The figure also shows that, as Re is increased, the shear stress of Ra ≤ 1000 has the same values for all investigated values of Re > 300. Fig. 7 shows the shear stress acting on the hot inner cylinder as a function of Re and Pr numbers at Ra=10^6. It can be observed that, for the same conditions of Ra, and Re, as Pr is increased, the shear stress is decreased due to the increase of the inertia forces against the buoyancy forces. For example, for Ra =10^6, and Re =100, however, the Richardson number (Rc) for Pr =0.1, 1, 5, and 10 are 1000, 100, 20, and 10 respectively. In other words, as Pr is increased, the shear stress is decreased due to the decrease of order of magnitude between the buoyancy forces and the inertia forces.

3.2. Heat transfer results and discussions

Samples of the characteristics of streamlines, isotherms, and local circumferential Nu distribution are presented in fig. 8. Through these figures, Pr is kept constant and equal to 5. For slightly low Ra, figs. 8-a to 8-c, with increasing speed of rotation, the thermal plumes move in the opposite direction of rotation. Conversely, with further increase of Re, the thermal plume direction is reversed and is tilted in the same direction of cylinder's rotation. In general, the forced flow tends to stratify the temperature field in the radial direction as the flow pattern is transferred from two eddies to one eddy pattern. Lastly, for no eddy flow pattern, the isotherms of the flow constitute concentric circles. These phenomena appear for all values of Pr. With increasing Ra, as Re is increased, we can find similar characteristics as those mentioned above. With further increase in Re, the iso-

therms are stratified, but don't convert to concentric circles due to the high buoyancy force which competes with the forced convection and keeps the flow pattern in the region of one eddy.

3.2.1. The local Nusselt number

The circumferential variation of the local Nu is shown in fig. 8. With increasing Re, the values of the points of minimum Nu values increase, and the points of maximum Nu decrease. For high Ra (Ra =500000), however, as Re is increased, two minimums and two maximums are also observed in the local Nu distribution around the inner cylinder. It is to be noted that, this phenomena occurs when the eddy in the right portion is very week, and moves towards disappearance due to the increased drag of the strong eddy at the left portion. With further increase of Re, the second peak disappears. For slightly low Rayleigh number, as Re is increased, the local Nu for both inner, and outer cylinders attains a nearly straight lines. This phenomena occurs for the flow in the pattern of no eddy.

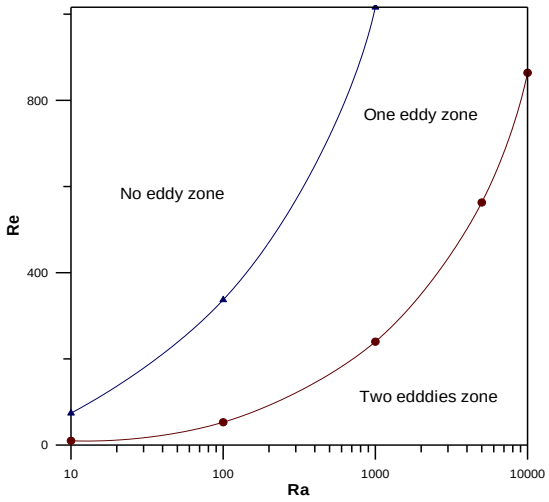

(a) Pr =0.1

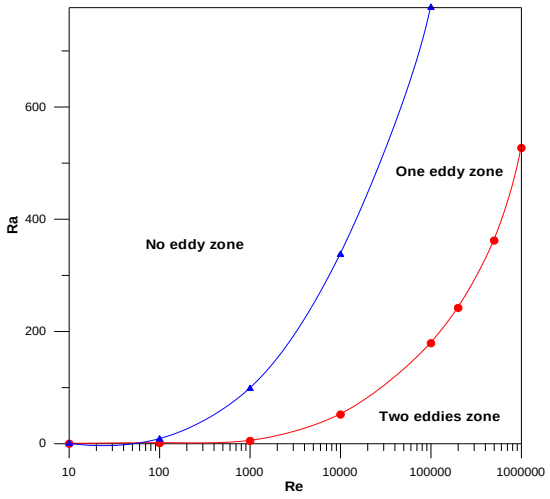

(b) Pr =10

Fig. 5. Classification of flow regimes according to the number of eddies on the (Ra-Re) plane when $\sigma = 2$.

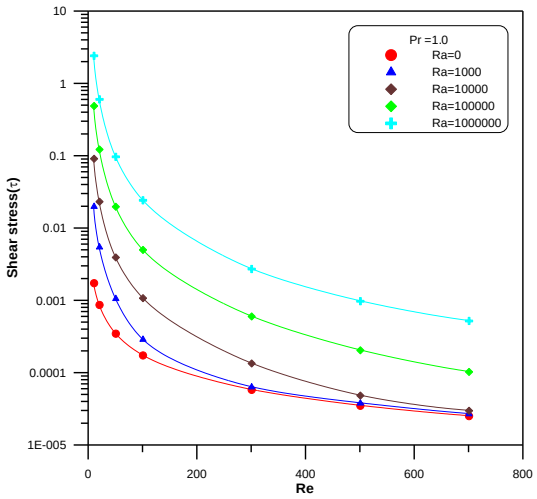

Fig. 6. Shear stress acting on the inner cylinder as a function of Re for several Ra, Pr =1, and σ =2.

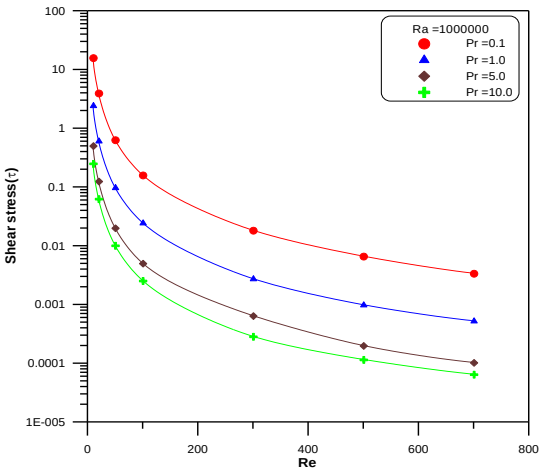

Fig. 7. Shear stress acting on the inner cylinder as a function of Re for several Pr, Ra=10^6, and σ =2.

3.2.2. The average Nusselt number

The average Nu for the combined convection between two horizontal concentric cylinders with a cooled rotating outer cylinder is calculated using eq. (9). The relation between the average Nu and the Re for different Ra is plotted in fig. 9. For small Pr, say Pr=0.01, fig. 9-a shows that, there is no effect of increasing Re on the value of the average Nu, so the average Nu has nearly a constant value which depends on Ra. As the diffusion of momentum is increased, for 0.1≤ Pr ≤ 10, the forced flow tends to stratify the temperature field in the radial direction. There is a kind of competition between the buoyancy induced flow and the forced flow. For Pr = 1.0, fig. 9-b shows that, for small Re, the average Nu is nearly identical to that of free convection, but above a certain Re it decreases rapidly. The range of Re where there is no great variation in heat transfer becomes wide as Ra increases, indicating the stronger role of the buoyancy forces. With further increase in Re, the average Nu experiences a change in slope as the flow pattern changes from one eddy to no eddy. In addition, for Ra=10000, when Rc is being from ∞ to 4, the average Nu is nearly identical to that of free convection With increasing inertia forces(i.e. decreasing Ri to less than 4), the average Nu curve' starts to decrease rapidly until the point of Ri equal to 0.0107. With further increase in inertia forces(i.e. Rc equals or less than 0.0107), the average Nu attains a constant value which depends on σ.

As Pr is increased, the diffusion of momentum is increased which increases the effect of the inertia forces against the buoyancy forces. It is noticed that as Ra is increased, the slope of the average Nu curves increases as the Re is increased for Ra ≤ 10^4 because of the increase in the inertia forces which makes a damping operatin to the buoyancy forces. For Ra ≥ 10^5, the average Nu curve has a constant slope as Re is increased. It is to be noted also that, for high Ra, and high Pr, with very small Re, there is a very little increase in the average Nu number due to the fact that, the diffusion of heat becomes more taster than the diffusion of momentum which increases the average Nu as Re is increased.

From fig. 9 the values of average Nu in terms of Ra, Re, and Pr were correlated as:

$$NU_i = 0.166 Ra^{0.336}\ Pr^{-0.008}\ Re^{-0.1263}\ . \qquad (13)$$

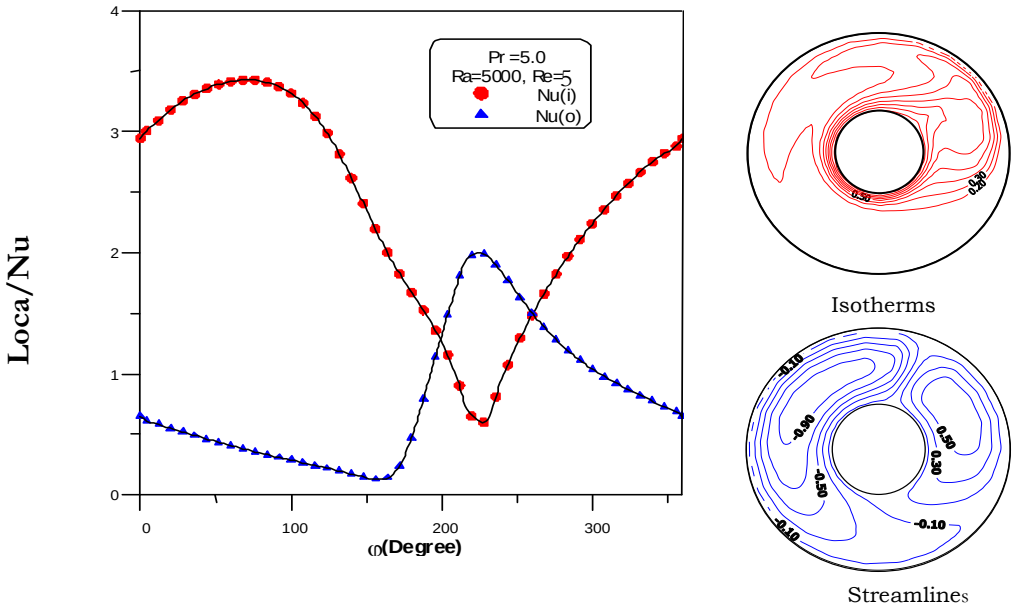

Fig. 8-a. Streamlines, isotherms, and local nusselt number circumferential distribution Ra=5000, Re=5, σ =2, and Pr =5.

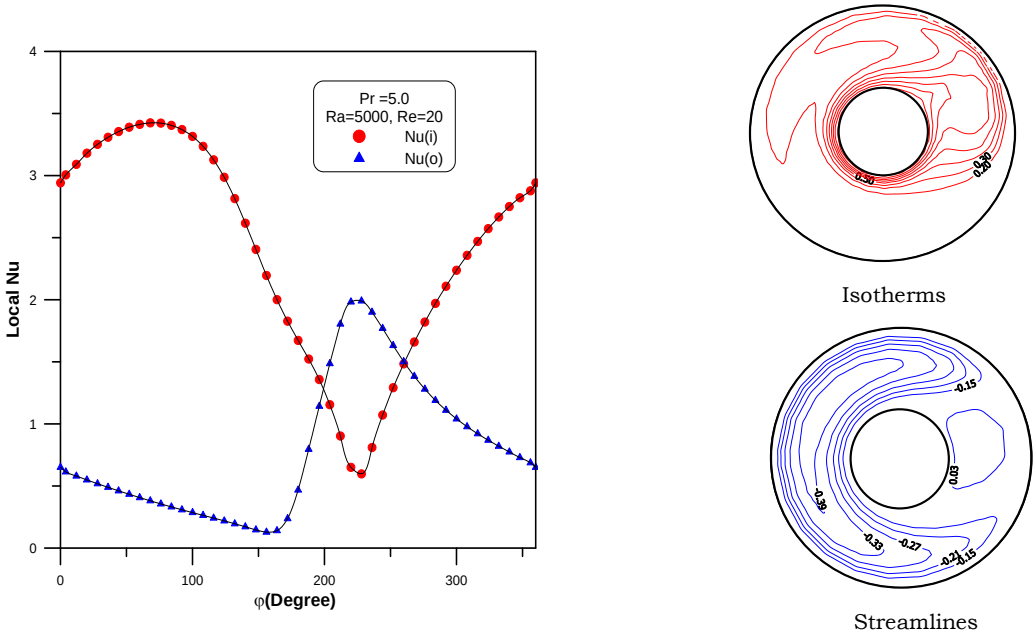

Fig. 8-b. Streamlines, isotherms, and local nusselt number circumferential distribution Ra=5000, Re=20, σ =2, and Pr =5.

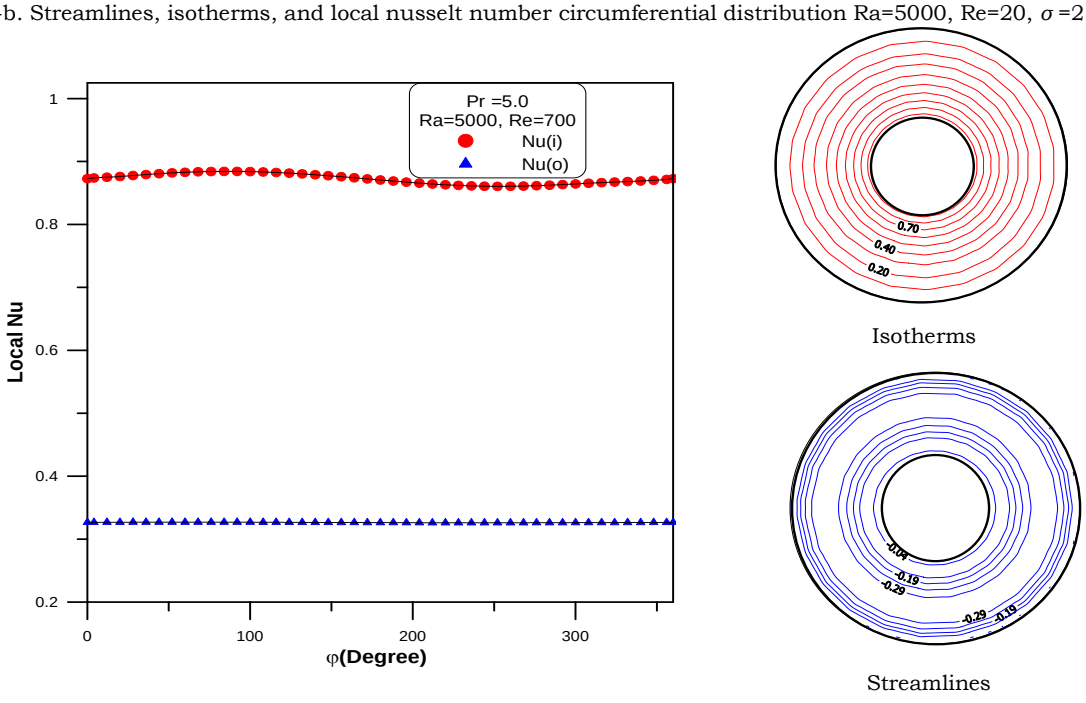

Fig. 8-c. Streamlines, isotherms, and local nusselt number circumferential distribution Ra=5000, Re=700, σ=2, and Pr=5.

The above correlation is valid for: $10^3 \leq Ra \leq 10^6$, $0.0 \leq Re \leq 2000$, $0.01 \leq Pr \leq 10.0$, and $\sigma = 2.0$. The maximum error was within 15%.

From fig. 9, it can be seen that for values of $Pr \geq 0.1$, and for $Ra \leq 10^4$, as Re is increased, the average Nu decreases rapidly in the regimes of two eddies, and one eddy patterns. With further increase in Re, the curve of the average Nu starts to attain a constant value due to the transfer of flow pattern from one eddy to no eddy.

4. Comparison of the Nusselt number results

A comparison of the present results for the average Nu values with those given by Joo-Sik Yoo [15] was made and illustrated in fig. 10 for Pr =0.7. Yoo used in his investigation a different definition to calculate the mean Nu as follows:

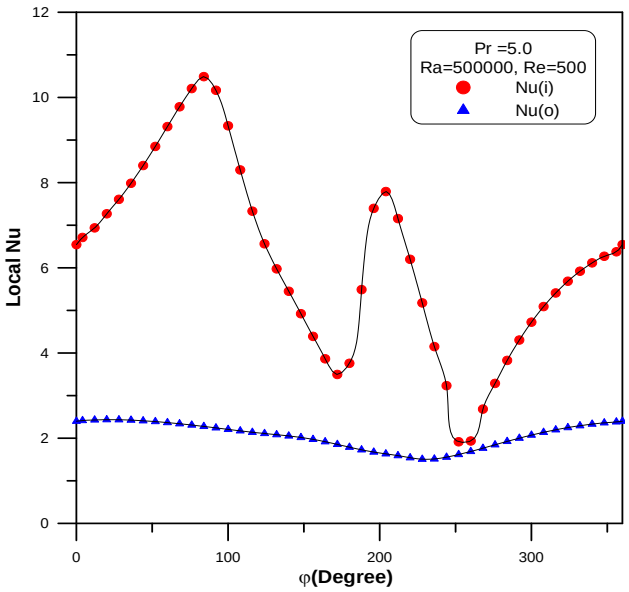

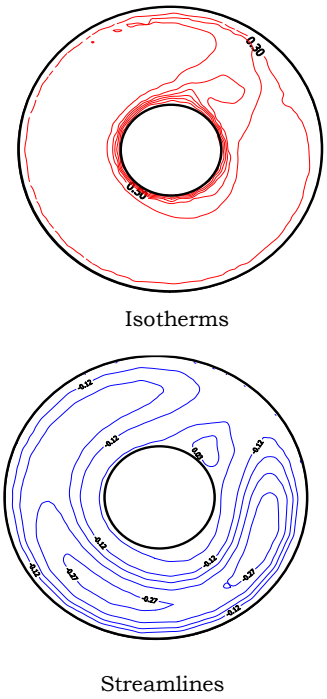

Fig. 8-d. Streamlines, isotherms, and local nusselt number circumferential distribution Ra=500000, Re=500, σ=2, and Pr=5.

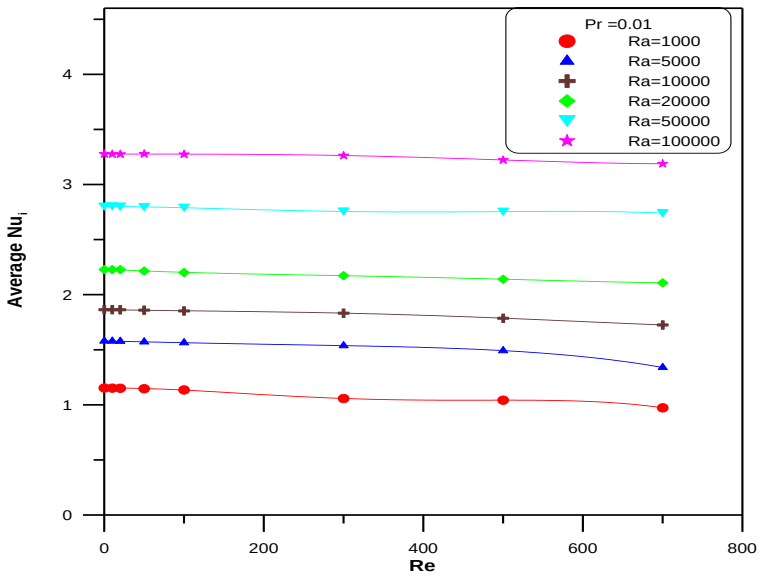

Fig. 9-a. Average Nu as a function of Re for Pr =0.01, and σ =2.

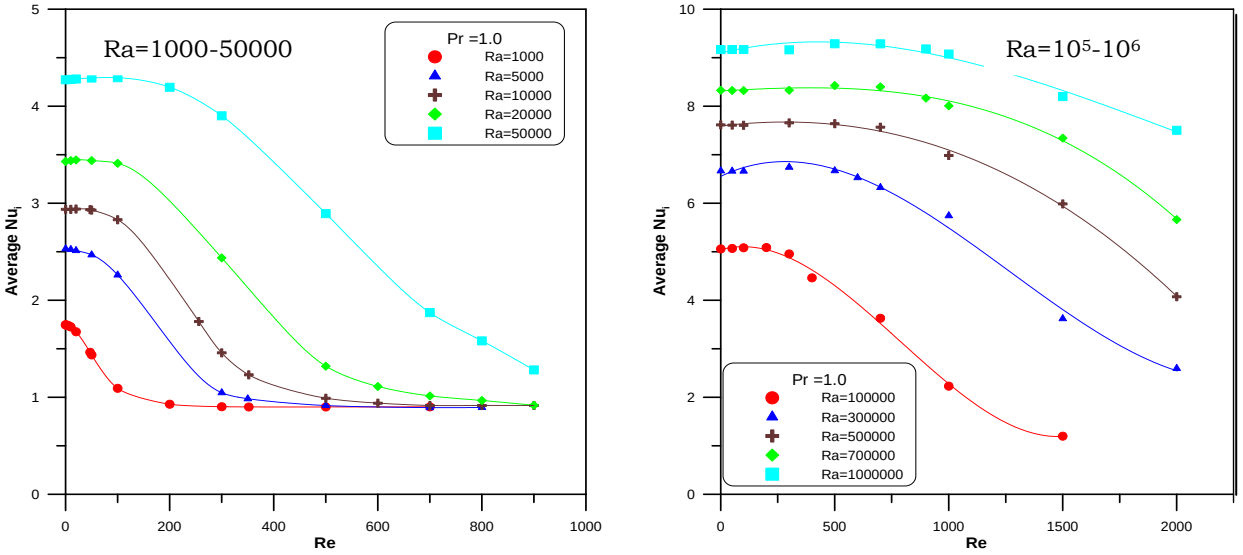

Fig. 9-b. Average Nu as a function of Re for Pr =1.0, and σ =2.

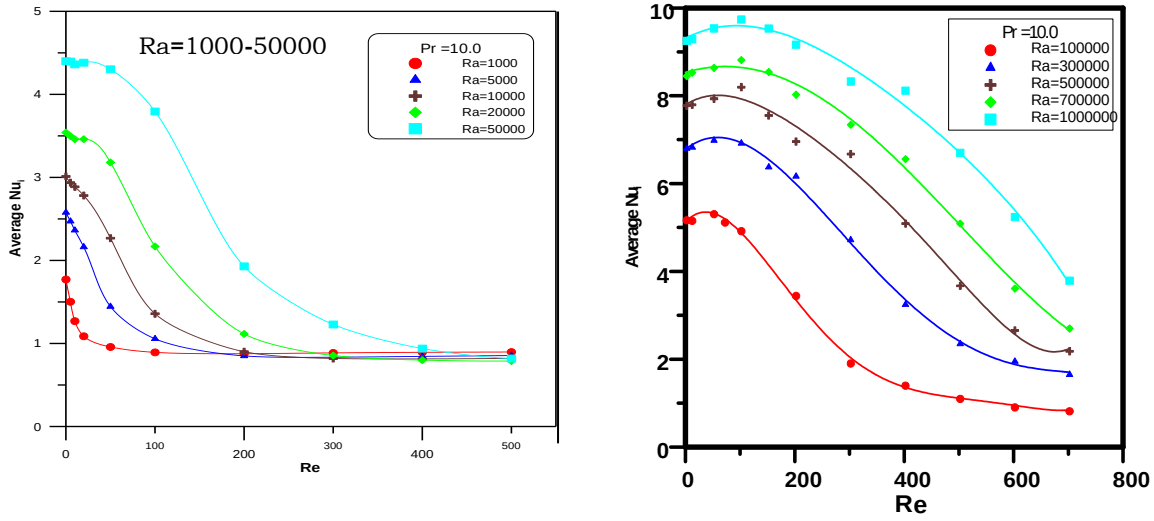

Fig. 9-c. Average Nu as a function of Re for Pr =10.0, and σ =2.

$$Nu = (Nu_i + Nu_o)/2 \ . \qquad (14)$$

So, in our present work, the mean Nusselt number is recalculated using eqs. (9 and 10) to enable us to make the necessary comparison with his results. As shown in fig. 10, the values of mean Nusselt number obtained from present work are higher than those obtained by Yoo. It is noticed that at a certain value of Re, there is a flat tail or departure in the curves obtained by Yoo. This behavior is experienced with the three values of Re (315, 400, and 700), but in our study this phenomenon didn't appear. The comparison was made at three values of Ra 10000, 20000. and 50000. As shown in fig. 10, as Ra increases, there is a wide agreement of data between Yoo and present work.

5. Conclusions

Mixed convection between two concentric horizontal cylinders is numerically investigated. The outer cylinder is isotherm at low temperature, and rotates about its axis with

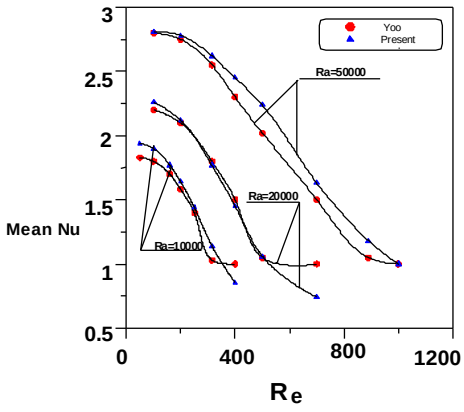

Fig. 10. Relation between mean Nusselt number, and Reynolds number for air (Pr = 0.7) between two horizontal concentric cylinders with a cooled rotating outer cylinder.

constant angular speed. The inner cylinder is isotherm at high temperature, and fixed. There are three flow patterns which can be classified according to the number of eddies as: two eddies, one eddy, and no eddy.

1. For very small Pr, there is no effect of increasing Re on the average Nu with respect to Ra, and σ, and the flow patterns tend to move from two eddies towards one eddy with increasing Re.
2. With increasing Pr, however, the average Nu has a constant value as Re in increased in the region of dominated free convection (i.e. when Rc is between ∞ and 4) until the thermal transitional Re, then the average Nu starts to decrease in the region of mixed convection.
3. With increasing Re, the average Nu curve starts to attain a straight line as Re reaches the value of the hydrodynamic critical Re between one eddy and no eddy in the region of dominated forced convection.
4. It can be noted that, as Pr increases, the slope of the curves of average Nu increases as Re is increased for the same value of Ra due to increasing the diffusion of momentum against the diffusion of heat, and also due to increasing of the inertia forces against the buoyancy forces.
5. The values of average Nu for the investigated ranges of Pr, Ra, and Re, are correlated as given in eq. (13).
6. A relationship between sheer stress (τ) acting on the inner heated cylinder, and Re is investigated.

As Ra increases, the sheer stress increases due to the increasing drag. Also, as Pr increases, the sheer stress decreases due to the increase in inertia forces against the buoyancy forces (i.e. decreasing Rc) which decreases the sheer stress.

Nomenclature

C	is the specific heat, J/Kg K,
d_i, d_o	are the diameters of inner and outer cylinders, respectively, m,
D_i, D_o	are the dimensionless diameters of inner and outer cylinders, respectively,
e_r, e_φ	are the unit vectors in the radial and angular directions, respectively,
g	is the acceleration of gravity, m/s^2,
Gr	is the Grashof number, $Gr = g\beta(T_i-T_o)L^3/\gamma^2$,
Gr_m	is the modified Grashof number, $Gr_m = 1/8[(\gamma_o/\gamma_i)^{1/2} ln(r_o/r_i)]^3 Gr_D$,
Gr_D	is the Grashof number based on the inner diameter, $Gr_D = g\beta(T_i-T_o)d_i^3/\gamma^2$,
h_i , h_o	are the average heat transfer coefficients at inner, and outer cylinders respectively, W/m^{2}K,
h_φ	is the local heat transfer coefficient at angle φ, W/m^{2}K.
K	is the fluid thermal conductivity, W/m K,
L	is the gap width of annulus, $(r_o - r_i)$, m,
Nu(i),Nu(o)	are the local Nusselt numbers at the inner and outer cylinders respectively,
Nu_i, Nu_o	are the average Nusselt numbers at the inner and outer cylinders respectively,
Nu	is the mean Nusselt number, $Nu=(Nu_i+ Nu_o)/2$,
p	is the pressure, N / m^2,
P^*	is the dimensionless pressure, $P^*= p/\rho U^2$,
Pr	is the Prandtl number, Pr = μC/K,
r	is the radial coordinate, m,
R	is the dimensionless radial coordinate, r/L,
r_i, r_o	are the radii of the inner and outer cylinders respectively, m.,

R_i, R_o are the dimensionless radii of the inner and outer cylinders, respectively, r_i / L, r_o / L,

Ra is the Ra yleigh number based on the gap width, Ra= Gr * Pr = $g\beta(T_i - T_o)L^3/a\gamma^2$,

Re is the pure forced convection Reynolds number, Re= $r_o \Omega_o L/ \gamma$,

Rc is the Richardson number, Gr /Re^2, or Ra/ Pr. Re^2,

T is the temperature, K,

T_i, T_o are the temperatures at the inner and outer cylinders respectively, K,

ΔT is the temperature difference, $(T_i - T_o)$, K,

t is the shear stress acting on the inner hot fixed cylinder, $t = \mu \frac{\partial \upsilon_\varphi}{\partial r}$, N/m^2,

U is the reference velocity, $r_o \Omega_o$, m/s,

υ_r , υ_φ are the velocity components in the radial and angular directions respectively, m/s,

u , v are the dimensionless velocity components in the radial and angular directions, respectively, ($u = \upsilon_r/U$ & $v = \upsilon_\varphi/U$), and

V is the dimensionless velocity vector.

Greek symbols

β is the coefficient of thermal expansion, K^{-1}.,

α is the thermal diffusivity, m^2/s.,

θ is the dimensionless temperature, $(T - T_o) / (T_i - T_o)$,

γ is the kinematic viscosity, m^2/s.,

ρ is the local fluid density, Kg/m^3,

ρ_i , ρ_o are the fluid density at the surfaces of inner, and outer cylinders, respectively, Kg/m^3.,

γ_i , γ_o are the kinematic viscosity at the inner, and outer cylinders respectively,

τ is the dimensionless shear stress, $\tau = t / \rho U^2$,

σ is the ratio of the inner cylinder diameter to gap width, $\sigma = d_i / L$.

ϕ is the angular coordinate, rad ,

φ is the angle being measured counter clock-wise from the upward vertical through the center of the annulus, rad,

Ω_o is the angular velocity of the outer cylinders, rad/s, and

μ is the dynamic viscosity, kg/m.s.

References

[1] W. Beckmann, Die Warmeuberstrangung in Zylindrischen Grasshichten bei Naturlicher Konvektion., Forschung 2. bd. 5, pp. 165-178 (1931).

[2] M. Iton, T. Fujita, N. Nishiwaki and M. Hirata., "A New Method of Correlating Heat Transfer Coefficient for Natural Convection in Horizontal Cylindrical Annuli," International Journal of Heat and Mass Transfer, Vol. 13, pp. 1364-1368 (1970).

[3] T.H. Kuehn and R.J. Goldstein, "Correlating Equations for Natural Convection Heat Transfer Between Horizontal Circular Cylinders," International Journal of Heat and Mass Transfer, Vol. 19, pp. 1127-1134 (1976).

[4] S.N. Singh and J.M. Elliott., "Free Convection Between Horizontal Concentric Cylinders in a Slightly Thermally Stratified Fluid," International Journal of Heat and Mass Transfer, Vol. 22, pp. 639-646 (1979).

[5] Y.T. Tsui and B. Tremblay, "On Transient Natural Convection Heat Transfer in Annulus Between Concentric Horizontal Cylinders with Isothermal Surfaces," International Journal of Heat and Mass Transfer, Vol. 27, pp. 103-111 (1984).

[6] Y.F. Rao, Y. Miki, K. Fukuda, Y. Takata and S. Hasegawa, "Flow Patterns of Natural Convection in Horizontal Cylindrical Annuli," Journal of Heat and Mass Transfer, Vol. 28, pp. 705-714 (1985).

[7] M. Prud Homme, L. Robillard and P. Vasseur, "A Steady of Laminar Natural Convection in a Non Uniformly Heated Annular Fluid Layer," International Journal of Heat and Mass Transfer, Vol. 30, pp. 1209-1222 (1987).

[8] V. T. Morgan., The Overall Convection Heat Transfer From Smooth Circular Cylinders, In Advances in Heat Transfer (Edited by T.F. Irvine and J.P. Hartnett), Vol. 11, pp. 199-265. Academic Press, New York (1975).

[9] R. Kumar., "Study of Natural Convection in Horizontal Annuli," Journal of Heat and Mass Transfer, Vol. 31, pp. 1137-1148 (1988).

[10] P.M. Kolsenikov and V.I. Bubnovich, "Non-Stationary Conjugate Free Convection Heat Transfer in Horizontal Cylindrical Coaxial Channels," International Journal of Heat and Mass Transfer, Vol. 31, pp. 1149-1156 (1988).

[11] Ho, C. J., and Y.H. Linh, "Laminar Natural Convection of Cold Water Enclosed in A Horizontal Annulus With Mixed Boundary Conditions," International Journal of Heat and Mass Transfer, Vol. 31, pp. 2113-2121 (1988).

[12] Joo-Sik Yoo. Transition and multiplicity of flows in natural convection in a narrow horizontal cylindrical annulus : Pr =0.4. International Journal of Heat and Mass Transfer, Vol. 42, 709-722 (1999).

[13] Joo-Sik Yoo. Natural convection in a narrow horizontal cylindrical annulus : Pr < 0.3. International Journal of Heat and Mass Transfer, Vol. 41, 3055-3073 (1998).

[14] Joo-Sik Yoo. Prandtl number effect on bifurcation and dual solution in natural convection in a horizontal annulus. International Journal of Heat and Mass Transfer, Vol. 42, pp. 3279-3290 (1999).

[15] Joo-Sik Yoo. Mixed convection of air between two horizontal concentric cylinders with a cold rotating outer cylinder. International Journal of Heat and Mass Transfer, Vol. 41, pp. 293-302 (1998).

[16] S.V. Patankar, Numerical Heat transfer and Fluid Flow, McGraw-Hill, New York (1980).

Received December 28, 2004
Accepted March 7, 2005